

Plasmon-enhanced Direct Detection of sub-MeV Dark Matter

Zheng-Liang Liang,^{1,*} Liangliang Su,^{2,†} Lei Wu,^{2,‡} and Bin Zhu^{3,§}

¹*College of Mathematics and Physics, Beijing University of Chemical Technology, Beijing, 100029, China*

²*Department of Physics and Institute of Theoretical Physics,
Nanjing Normal University, Nanjing, 210023, China*

³*School of Physics, Yantai University, Yantai 264005, China*

(Dated: January 23, 2024)

Plasmon, a collective mode of electronic excitation in semiconductor materials, provides a unique avenue for the detection of light dark matter (DM). In this work, we first generalize the theoretical formalism of plasmon to treat the relativistic DM particles. We demonstrate that the plasmon resonance effect for sub-MeV DM can be significantly enhanced, particularly in scenarios of boosted DM with a light mediator. Utilizing the first data from SENSEI at SNOLAB, we derive a new strong limit on the sub-MeV DM-electron scattering cross section, which is more stringent than those from liquid detectors.

INTRODUCTION

Dark matter, constituting approximately 85% of the Universe's mass, plays a crucial role in the structure formation and evolution of our Universe. Despite the overwhelming astrophysical and cosmological evidence confirming its existence, the nature of dark matter remains elusive. The Weakly Interacting Massive Particle (WIMP) hypothesis has been a leading contender, yet recent null results from WIMP searches [1–3] have prompted extensive exploration of alternative possibilities, particularly focusing on sub-GeV dark matter [4–19]. Given that the nuclear recoil of light dark matter falls below the threshold of conventional detectors, great efforts have focused on utilizing ionization signals to extend sensitivity in direct detection experiments.

The sub-GeV DM particles with the coupling to the electrons can be detected in semiconductor targets, such as SENSEI [20], DAMIC [21], EDELWEISS [22], CDEX [23] and SuperCDMS [24]. The density functional theory (DFT) method was first introduced in the description of the DM-electron in semiconductors [25], and have been further extended to a broader range of target materials [26–40]. Other methodologies are still under development [41–45]. For example, the dielectric function that accounts for the screening has been incorporated into the formalism describing the DM-electron interaction in semiconductor targets [46–48]. On the other hand, a collective excitation mode of the valence electrons in solid materials known as the plasmon has been considered as a possible explanation of the excess observed in several semiconductor detectors [46, 49] and included in the direct detection [50–53].

In this work, we focus on the plasmon excitation induced by the interaction between the accelerated DM and the semi-conductor detectors. One key observation is that if light DM particle move fast enough, it can excite the plasmon in silicon and germanium detectors, and the resonance behavior of the plasmon will significantly increase the ionization yield. To illustrate this,

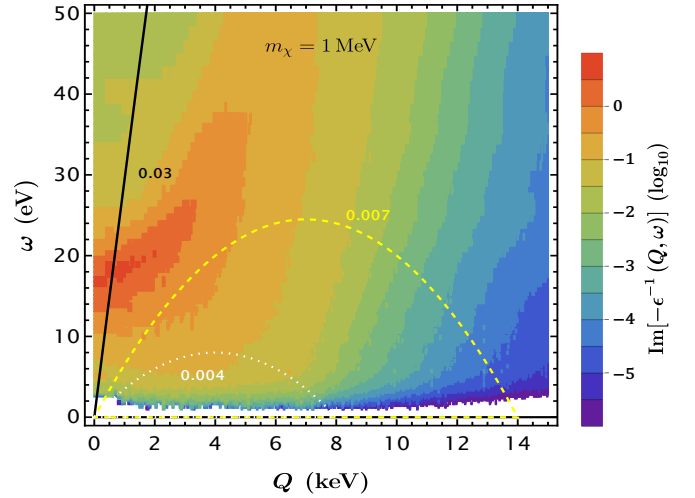


Figure 1. The ELF $\text{Im}[-\epsilon^{-1}(Q, \omega)]$ for silicon semiconductors, calculated with the DFT methods [46, 47]. The kinematically accessible phase spaces for a 1 MeV DM particle with incident velocities $v_\chi = 0.004c$, $0.007c$, and $0.03c$ are bounded by white dotted, yellow dashed and black solid line, respectively.

we show the energy loss function (ELF) $\text{Im}[-\epsilon^{-1}(Q, \omega)]$ for silicon on the plane of the transferred momentum Q and energy ω in Fig. 1, which is defined as the imaginary part of the inverse dielectric function $\epsilon(Q, \omega)$. Such ELF reflects the target material response to an external perturbation. A resonance structure corresponding to the plasmon excitation is clearly seen around the area ($Q < 5$ keV, $\omega \sim 15$ eV). Thus, for a 1 MeV DM particle, a minimum incident velocity $v_{\text{DM}} \gtrsim 10^{-2} c$ is required to excite a plasmon in the silicon targets, which is much higher than the typical velocity of DM in the Galactic halo. However, a fraction of DM particles in the Galactic halo could be up-scattered by energetic Cosmic-Ray

(CR) particles¹ [65–78], and trigger the plasmon signals in semiconductor targets. Especially in scenarios with a light mediator, the plasmon resonance pole appears in the lower momentum transfer Q region, which leads to an enhanced electronic excitation rate. As a demonstration, we present the sensitivity of the CRDM-electron scattering cross section by using the first data from the silicon detector SENSEI at SNOLAB. Our new bound is about two orders of magnitude stronger than that from the Xenon1T.

EXCITATION RATE INDUCED BY THE RELATIVISTIC DM PARTICLES

In semiconductor targets, the nonrelativistic DM-electron scattering process can be described using the ELF $\text{Im}(-\epsilon^{-1}(\mathbf{Q}, \omega))$. The ELF that naturally incorporates the many-body in-medium effects, including the screening and the plasmon resonance, can be evaluated with the first-principles methods based on the DFT [46, 49, 51].

As aforementioned, while the typical halo DM particles with velocity $v_{\text{DM}} \sim 10^{-3} c$ fall short of energy to directly excite a plasmon, a fraction that is up-scattered by the DM-CR interaction may obtain enough momentum to excite plasmons via the DM-electron scattering in silicon and germanium detectors. Here we discuss how to calculate the excitation rates induced by the CRDM. As a benchmark scenario of CRDM, we consider the interaction between the DM particles (χ) and standard model particles (e.g., electrons) through the exchange of a dark photon A'_μ as follows

$$\mathcal{L}_{\text{int}} \supset g_\chi \bar{\chi} \gamma^\mu \chi A'_\mu + g_e \bar{e} \gamma^\mu e A'_\mu, \quad (1)$$

where g_χ and g_e are the coupling constants for the dark photon-DM particle and dark photon-electron interactions, respectively.

Since we are only interested in the electronic excitation energy below 100 eV, in which case the electrons in the semiconductor is still nonrelativistic. Therefore, we need to rewrite the dark photon-electron Lagrangian in the framework of nonrelativistic effective field theory (EFT) [52] as follows,

$$\mathcal{L}_e^{\text{eff}} \supset g_e A'_0 \psi_e^* \psi_e + \frac{ig_e}{2m_e} \mathbf{A}' \cdot (\psi_e^* \vec{\nabla} \psi_e - \psi_e^* \overleftarrow{\nabla} \psi_e) + \dots, \quad (2)$$

where ψ_e is the nonrelativistic electron wavefunction. Only the first term $g_e A'_0 \psi_e^* \psi_e$ is relevant for our purpose because the second term (electric current) and beyond

are suppressed by the electron mass m_e for the electron bound state wavefunction.

On the other hand, the CRDM component remains relativistic. Thus, the cross section of the process in which the valence electrons bound to the fixed semiconductor target is excited from the initial state $|i\rangle$ to the final one $|f\rangle$ by a DM particle is written as

$$\sigma_{i \rightarrow f} = \int \frac{d^3 p'_\chi}{(2\pi)^3} \frac{|\overline{\mathcal{M}}_{i \rightarrow f}|^2}{4E_\chi E'_\chi v_\chi} 2\pi \delta(\omega_{pp'} + \varepsilon_i - \varepsilon_f), \quad (3)$$

where $E_\chi(E'_\chi)$ and $\varepsilon_i(\varepsilon_f)$ represent the energies of initial (final) DM and target states, respectively; $\omega_{pp'} = E_\chi - E'_\chi$ is energy loss of the DM particle. The scattering amplitude $\mathcal{M}_{i \rightarrow f}$ is defined by the T -matrix

$$\begin{aligned} \langle \mathbf{p}'_\chi, f | iT | \mathbf{p}_\chi, i \rangle &= i \mathcal{M}_{i \rightarrow f} 2\pi \delta(\omega_{pp'} + \varepsilon_i - \varepsilon_f) \\ &= \bar{u}_{p'_\chi}^{s'} \gamma^0 u_{p_\chi}^s \frac{i g_\chi g_e}{Q^2 - (\varepsilon_f - \varepsilon_i)^2 + m_{A'}^2} \\ &\quad \times \langle i | e^{i\mathbf{Q} \cdot \hat{\mathbf{x}}} | f \rangle 2\pi \delta(\omega_{pp'} + \varepsilon_i - \varepsilon_f), \end{aligned} \quad (4)$$

where $Q = |\mathbf{Q}| = |\mathbf{p}_\chi - \mathbf{p}'_\chi|$ denotes the momentum transferred to the target, and $u_{p_\chi}^s$ and $\bar{u}_{p'_\chi}^{s'}$ represent the spinors of the initial and final DM particles, respectively. In the above derivation, the contribution of $q_\mu q_\nu$ term (with q^μ being the 4-momentum transfer) from the massive vector propagator is cancelled because of the conservation condition of vector current at the DM-dark photon vertex.

Thus, after averaging over the initial, and summing over the final target states, the total cross section of DM-semiconductor scattering can be written as

$$\begin{aligned} \sigma &= \sum_{i,f} \mathcal{P}_i \sigma_{i \rightarrow f} \\ &= 2N_{\text{cell}} V_{\text{cell}} \frac{\pi \bar{\sigma}_{\chi e}}{\mu_{\chi e}^2} \int d\omega \int \frac{d^3 \mathbf{Q}}{(2\pi)^3} \frac{(E_\chi + E'_\chi)^2 - Q^2}{4E_\chi E'_\chi v_\chi} \\ &\quad \times \frac{\delta(\omega_{pp'} - \omega)}{V_{\text{Cou}}(\mathbf{Q})} \left(\frac{\alpha^2 m_e^2 + m_{A'}^2}{Q^2 - \omega^2 + m_{A'}^2} \right)^2 \text{Im} \left[\frac{-1}{\epsilon(\mathbf{Q}, \omega)} \right], \end{aligned} \quad (5)$$

where \mathcal{P}_i denotes the thermal distribution of the initial target state $|i\rangle$. V_{cell} is the volume of the unit cell, with $2\pi^2/(\alpha m_e^2 V_{\text{cell}}) = 2.0$ eV for silicon, $N_{\text{cell}} = M_{\text{target}}/M_{\text{cell}}$ represents the number of unit cells in the target materials, where $M_{\text{cell}} = 2m_{\text{Si}} = 52.33$ GeV for silicon, and $V_{\text{Cou}}(\mathbf{Q}) = 4\pi\alpha/Q^2$ describes the Coulomb interaction of electron in momentum space.

With Eq. 5, the differential electronic excitation rate induced by the CRDM per unit mass in (silicon) detector can be expressed as

¹ Other fast-moving light DM possibilities, such as the boosted dark matter (BDM) [54–57], the atmospheric dark matter [10,

$$\begin{aligned}
\frac{dR}{d\omega} &= \frac{1}{M_{\text{target}}} \int dE_\chi \int \frac{d\Omega}{4\pi} \frac{d\Phi_\chi}{dE_\chi} \frac{d\sigma}{d\omega} \\
&= \frac{1}{\rho_T} \frac{\bar{\sigma}_{\chi e}}{4\alpha\mu_{\chi e}^2} \int \frac{d^3\mathbf{Q}}{(2\pi)^3} \int dE_\chi \frac{d\Phi(E_\chi)}{dE_\chi} \left(\frac{(2E_\chi - \omega)^2 - Q^2}{4E_\chi(E_\chi - \omega)} \right) \left(\frac{\alpha^2 m_e^2 + m_{A'}^2}{Q^2 - \omega^2 + m_{A'}^2} \right)^2 \left(\frac{E_\chi(E_\chi - \omega)}{p_\chi^2} \right) \\
&\times Q \text{Im} \left[\frac{-1}{\epsilon(\mathbf{Q}, \omega)} \right] \Theta \left[E_\chi - \sqrt{(p_\chi - Q)^2 + m_\chi^2} - \omega \right], \tag{6}
\end{aligned}$$

where $\rho_T = N_{\text{cell}} V_{\text{cell}} / M_{\text{target}}$ is the target density, and Θ is the Heaviside step function. The factor $1/4\pi$ stems from the assumption of a homogeneous CRDM flux. In this work, we adopt the ELF $\text{Im}[-\epsilon^{-1}(\mathbf{Q}, \omega)]$ from the *DarkELF* package [47]. More details on the calculation can be found in the supplemental material. $d\Phi_\chi/dE_\chi$ is the flux of CRDM.

The CR-DM interaction can accelerate the nonrelativistic light DM in our galaxy to a (semi-) relativistic speed. Here we calculate the flux of such CRDM due to the DM-electron scattering in local interstellar (LIS) $d\Phi_e^{\text{LIS}}/dT_e$ [79] with the following formula,

$$\begin{aligned}
\frac{d\Phi_\chi}{dT_\chi} &= \sum_i \int \frac{d\Omega}{4\pi} \int_{\text{l.o.s.}} ds \int_{T_e^{\text{min}}}^\infty dT_e \frac{\rho_\chi}{m_\chi} \frac{d\sigma_{\chi e}}{dT_\chi} \frac{d\Phi_e^{\text{LIS}}}{dT_e} \\
&\equiv D_{\text{eff}} \frac{\rho_\chi^{\text{local}}}{m_\chi} \int_{T_e^{\text{min}}}^\infty dT_e \frac{d\sigma_{\chi e}}{dT_\chi} \frac{d\Phi_e^{\text{LIS}}}{dT_e}, \tag{7}
\end{aligned}$$

where $\rho_\chi^{\text{(local)}} = 0.4 \text{ GeV}$ is the local DM halo density. In this work we adopt the Navarro-Frenk-White (NFW) DM profile and obtain an effective distance $D_{\text{eff}} \equiv \frac{1}{4\pi\rho_\chi^{\text{local}}} \int_{\text{l.o.s.}} \rho_\chi ds d\Omega = 8.02 \text{ kpc}$ after performing the full line-of-sight integration out to 10 kpc under the assumptions of a homogeneous CR flux.

In the rest frame of a DM particle, its differential scattering cross section with a free electron can be obtained with

$$\begin{aligned}
\frac{d\sigma_{\chi e}}{dT_\chi} &= \frac{\bar{\sigma}_{\chi e} (\alpha^2 m_e^2 + m_{A'}^2)^2}{4\mu_{\chi e}^2 (2m_e T_e + T_e^2) (2m_\chi T_\chi + m_{A'}^2)^2} [m_\chi T_\chi^2 \\
&+ 2m_\chi (m_e + T_e)^2 - T_\chi ((m_e + m_\chi)^2 + 2m_\chi T_e)], \tag{8}
\end{aligned}$$

where a reference cross section

$$\bar{\sigma}_{\chi e} \equiv \frac{\mu_{\chi e}^2}{\pi} \left(\frac{g_\chi g_e}{\alpha^2 m_e^2 + m_{A'}^2} \right)^2, \tag{9}$$

defined at a benchmark momentum transfer αm_e is introduced to parameterize the DM-electron coupling strength, with $\alpha = e^2/4\pi$ being the electromagnetic fine structure constant, $m_{A'}$ being the dark photon mass, m_e and $\mu_{\chi e}$ being the electron and reduced mass of DM-electron pair, respectively. To boost a DM particle to a

recoil energy T_χ requires the incident CR electron has a kinetic energy larger than

$$T_e^{\text{min}} = \left(\frac{T_\chi}{2} - m_e \right) \left[1 \pm \sqrt{1 + \frac{2T_\chi (m_e + m_\chi)^2}{m_\chi (2m_e - T_\chi)^2}} \right], \tag{10}$$

where \pm signs denote the case of $T_\chi > 2m_e$ and $T_\chi < 2m_e$, respectively. When $T_\chi = 2m_e$, $T_e^{\text{min}} = (m_e + m_\chi)\sqrt{m_e/m_\chi}$. In a parallel fashion we can also define the minimum kinetic energy T_p^{min} for a CR proton to produce a DM particle with recoil energy T_χ . It is noted that $T_p^{\text{min}} > T_e^{\text{min}}$ for a DM with T_χ , as shown in Fig. 2, the CRDM flux due to the proton-DM scattering can be neglected. Thus we only consider the CRDM boosted by the electrons in CRs.

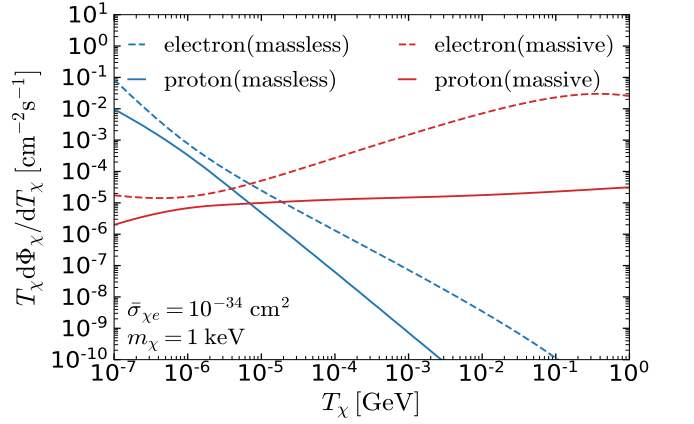


Figure 2. The CRDM flux as the function of T_χ from the proton-DM (solid lines) and electron-DM (dotted lines) scattering via a massless (blue lines) and massive (red lines) mediator, respectively. The cross section $\bar{\sigma}_{\chi e} = \mu_{\chi e}^2 \bar{\sigma}_{\chi p} / \mu_{\chi p}^2 = 10^{-34} \text{ cm}^2$ and DM mass $m_\chi = 1 \text{ keV}$ is adopted as the benchmark point.

NUMERICAL RESULTS AND DISCUSSIONS

By use of Eq. (6), now we are able to calculate the event rates $dR/d\omega$ induced by the CRDM in the semiconductor. In Fig. 3 shown are the differential rates for a 1 keV CRDM with a benchmark cross section $\bar{\sigma}_{\chi e} = 10^{-34} \text{ cm}^2$

in the massless (blue) and the massive (orange) mediator limit, respectively.

The plasmon resonance effect is clearly seen in Fig. 3 for both the massive and the massless mediator scenarios. As expected, such effect is particularly remarkable for the massless mediator case where the contribution from the small Q regime is optimally maximized. Similar resonance behavior in the massive mediator case has been observed in the solar-accelerated DM scenario [53], but the relevant enhancement is somewhat mild. So it is the first time that a remarkable plasmon resonance enhancement is observed in calculation based on a realistic fast DM source.

To translate the spectrum into observable electron signals, we adopt the model in Ref. [25], where the number of the secondary electron-hole pairs triggered by the primary one is described with the average energy for generating an electron-hole pair ε in high energy recoils. In this model, the ionization charge Q is given by

$$Q(\omega) = 1 + \lfloor (\omega - E_{\text{gap}}) / \varepsilon \rfloor, \quad (11)$$

where $\lfloor x \rfloor$ is the floor function, and E_{gap} represents the band gap of the semiconductor. For silicon semiconductors, we take $E_{\text{gap}} = 1.2 \text{ eV}$ and $\varepsilon = 3.8 \text{ eV}$.

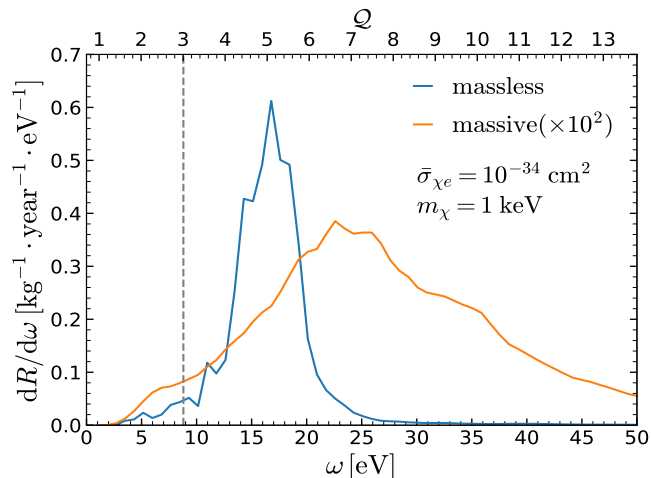


Figure 3. The differential event rates $dR/d\omega$ as a function of the deposited energy ω for 1 keV DM with a massless (blue) and a massive (orange) mediator, respectively. The grey dashed line marks the $Q \geq 3$ threshold adopted in our discussion. A benchmark DM-electron scattering cross section $\bar{\sigma}_{\chi e} = 10^{-34} \text{ cm}^2$ is assumed.

In Fig. 4, we illustrate the sensitivities of the SENSEI experiment with a 534.9 g · days exposure on the DM-electron cross section $\bar{\sigma}_{\chi e}$ for sub-MeV DM interacting with a massless (left panel) and massive (right panel) mediator, respectively. Considering the remarkable plasmon effect, we adopt a relatively higher threshold ($Q \geq 3$) and near-zero background event in the analysis to avoid

the noises in $1e^-$ and $2e^-$ bin. For the massless mediator, the exclusion limit on DM-electron scattering cross section $\bar{\sigma}_{\chi e}$ can be as large as about two orders of magnitude stronger than those drawn from the Xenon1T experiments with S2-only signal [81] (more details see the supplemental material).

In the massive mediator case, however, the sensitivity of semiconductor is losing advantage to the Xenon1T experiment due to the absence of the $1/Q^2$ enhancement factor, in addition to a small CRDM flux in the low energy regime. It is also observed that in the region $m_\chi \gtrsim 80 \text{ keV}$, the sensitivity of the semiconductor begins to improve compared to the Xenon experiments. This is because the event rates will be enhanced by the factor $E_\chi(E_\chi - \omega)/p_\chi^2 \sim 1/v_\chi^2$ for heavy DM with low kinetic energy, which can induce detectable signals in semiconductors but not in isolated atoms. For a massless mediator, this effect is canceled by the suppression of CRDM flux $d\Phi \propto d\sigma \sim 1/m_\chi$.

CONCLUSIONS

The nontrivial collective behaviors of the electrons in solid detectors such as screening and the plasmon excitation has proved important in the probe of the sub-MeV DM. In this paper, we discuss the prospect of detecting sub-MeV DM by utilizing the plasmon resonance effect in semiconductor detectors. While the kinetic condition of plasmon is demanding for the halo sub-GeV DM flux, those CR-accelerated DM particles are potentially able to excite plasmons in semiconductor targets. Our calculation shows that while the kinetically relevant parameter space begins to overlay the plasmon pole for the boosted DM flux, the excitation rates receive a significant enhancement particularly in the massless mediator scenario, owing to the DM form factor $1/Q^2$. To be specific, the differential event rates of CRDM-electron scattering is observed to have a resonance structure centered in the range of $10 \text{ eV} < \omega < 30 \text{ eV}$. After integrating out the differential rates above the threshold $Q \geq 3$, it is found that semiconductor detectors are more sensitive than the liquid detectors in the massless mediator scenario in the DM mass range $m_\chi \in [\text{keV}, \text{MeV}]$, while the liquid detectors overtake in the massive mediator case.

This finding encourages further discussions on other fast DM sources (e.g., the solar reflection DM flux [82]) in the attempt to extensively explore the uncharted DM parameter space in the sub-GeV DM mass range, by utilizing the plasmon resonance effect in the future semiconductor detectors, including the upgraded SENSEI, DAMIC-M and Oscura experiments [83].

Note Added When we finalize this manuscript, the paper [80] appears on arXiv, in which the sensitivity of solar reflection DM was discussed. As there was no avail-

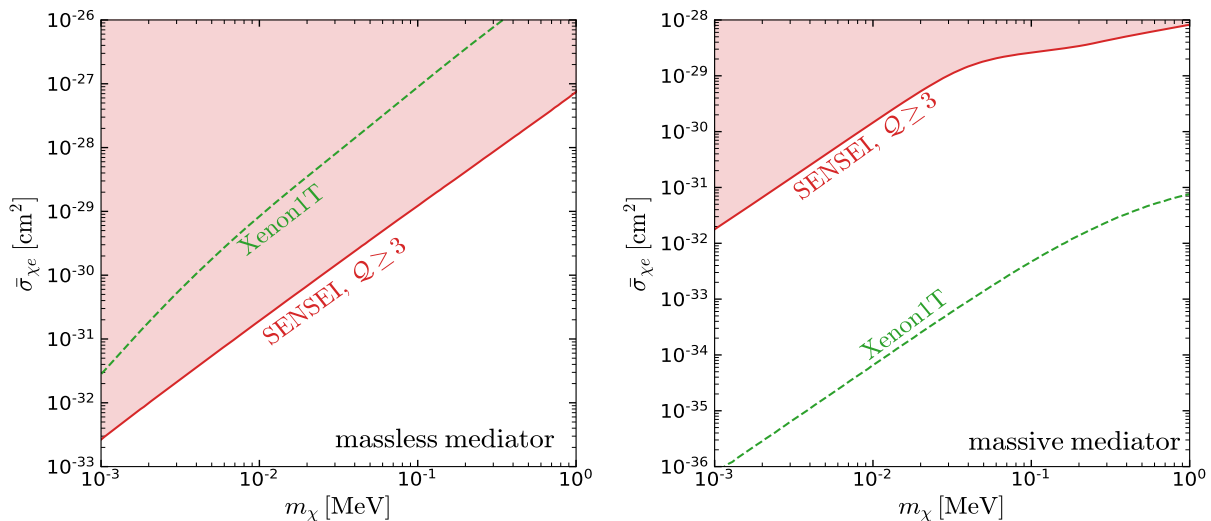


Figure 4. The upper limits on the DM-electron cross section $\bar{\sigma}_{\chi e}$ for massless (left) and massive (right) mediator. The red lines correspond to the 4 events with the threshold $Q \geq 3$ and a 534.9 g-days exposure of silicon detector from the SENSEI experiment at SNOLAB [80]. The green lines represent the constraints from Xenon1T experiments with S2-only signal [81].

able data during our writing, we had to update our previous results with new data. On the other hand, in our work, we explicitly present the consistent formalism to treat the relativistic DM, which was not seen in [80].

ACKNOWLEDGMENTS

This work is supported by the National Natural Science Foundation of China (NNSFC) under grants No. 12275134, No. 12275232, No. 12335005 and No. 12147228.

* liangzl@mail.buct.edu.cn

† liangliangsu@njnu.edu.cn

‡ leiwu@njnu.edu.cn

§ zhubin@mail.nankai.edu.cn

- [1] Q. Wang et al. (PandaX-II), *Chin. Phys. C* **44**, 125001 (2020), 2007.15469.
- [2] J. Aalbers et al. (LZ) (2022), 2207.03764.
- [3] E. Aprile et al. (XENON) (2023), 2303.14729.
- [4] R. Essig, J. Mardon, and T. Volansky, *Phys. Rev. D* **85**, 076007 (2012), 1108.5383.
- [5] Z. Z. Liu et al. (CDEX), *Phys. Rev. Lett.* **123**, 161301 (2019), 1905.00354.
- [6] T. Emken, R. Essig, C. Kouvaris, and M. Sholapurkar, *JCAP* **09**, 070 (2019), 1905.06348.
- [7] R. Essig, J. Pradler, M. Sholapurkar, and T.-T. Yu, *Phys. Rev. Lett.* **124**, 021801 (2020), 1908.10881.
- [8] T. Trickle, Z. Zhang, and K. M. Zurek, *Phys. Rev. D* **105**, 015001 (2022), 2009.13534.
- [9] E. Andersson, A. Bökmark, R. Catena, T. Emken, H. K. Moberg, and E. Åstrand, *JCAP* **05**, 036 (2020), 2001.08910.
- [10] L. Su, W. Wang, L. Wu, J. M. Yang, and B. Zhu, *Phys. Rev. D* **102**, 115028 (2020), 2006.11837.
- [11] S. E. Vahsen, C. A. J. O'Hare, and D. Loomba, *Ann. Rev. Nucl. Part. Sci.* **71**, 189 (2021), 2102.04596.
- [12] L. Su, L. Wu, and B. Zhu, *Phys. Rev. D* **105**, 055021 (2022), 2105.06326.
- [13] R. Catena, T. Emken, M. Matas, N. A. Spaldin, and E. Urdshals, *Phys. Rev. Res.* **3**, 033149 (2021), 2105.02233.
- [14] G. Elor, R. McGehee, and A. Pierce, *Phys. Rev. Lett.* **130**, 031803 (2023), 2112.03920.
- [15] H.-Y. Chen, A. Mitridate, T. Trickle, Z. Zhang, M. Bernardi, and K. M. Zurek, *Phys. Rev. D* **106**, 015024 (2022), 2202.11716.
- [16] R. Catena, D. Cole, T. Emken, M. Matas, N. Spaldin, W. Tarantino, and E. Urdshals, *JCAP* **03**, 052 (2023), 2210.07305.
- [17] J. Li, L. Su, L. Wu, and B. Zhu, *JCAP* **04**, 020 (2023), 2210.15474.
- [18] L. Su, L. Wu, N. Zhou, and B. Zhu, *Phys. Rev. D* **108**, 035004 (2023), 2212.02286.
- [19] W. Wang, W.-L. Xu, and J. M. Yang (2023), 2304.13243.
- [20] L. Barak et al. (SENSEI), *Phys. Rev. Lett.* **125**, 171802 (2020), 2004.11378.
- [21] N. Castelló-Mor (DAMIC-M), *Nucl. Instrum. Meth. A* **958**, 162933 (2020), 2001.01476.
- [22] Q. Arnaud et al. (EDELWEISS), *Phys. Rev. Lett.* **125**, 141301 (2020), 2003.01046.
- [23] Z. Y. Zhang et al. (CDEX), *Phys. Rev. Lett.* **129**, 221301 (2022), 2206.04128.
- [24] D. W. Amaral et al. (SuperCDMS), *Phys. Rev. D* **102**, 091101 (2020), 2005.14067.
- [25] R. Essig, M. Fernandez-Serra, J. Mardon, A. Soto, T. Volansky, and T.-T. Yu, *JHEP* **05**, 046 (2016), 1509.01598.
- [26] Y. Hochberg, Y. Zhao, and K. M. Zurek, *Phys. Rev. Lett.* **116**, 011301 (2016), 1504.07237.

- [27] R. Essig, J. Mardon, O. Slone, and T. Volansky, Phys. Rev. D **95**, 056011 (2017), 1608.02940.
- [28] Y. Hochberg, Y. Kahn, M. Lisanti, C. G. Tully, and K. M. Zurek, Phys. Lett. B **772**, 239 (2017), 1606.08849.
- [29] S. Derenzo, R. Essig, A. Massari, A. Soto, and T.-T. Yu, Phys. Rev. D **96**, 016026 (2017), 1607.01009.
- [30] S. Knapen, T. Lin, M. Pyle, and K. M. Zurek, Phys. Lett. B **785**, 386 (2018), 1712.06598.
- [31] S. Griffin, S. Knapen, T. Lin, and K. M. Zurek, Phys. Rev. D **98**, 115034 (2018), 1807.10291.
- [32] T. Trickle, Z. Zhang, and K. M. Zurek, Phys. Rev. Lett. **124**, 201801 (2020), 1905.13744.
- [33] N. A. Kurinsky, T. C. Yu, Y. Hochberg, and B. Cabrera, Phys. Rev. D **99**, 123005 (2019), 1901.07569.
- [34] T. Trickle, Z. Zhang, K. M. Zurek, K. Inzani, and S. M. Griffin, JHEP **03**, 036 (2020), 1910.08092.
- [35] B. Campbell-Deem, P. Cox, S. Knapen, T. Lin, and T. Melia, Phys. Rev. D **101**, 036006 (2020), [Erratum: Phys.Rev.D 102, 019904 (2020)], 1911.03482.
- [36] A. Coskuner, A. Mitridate, A. Olivares, and K. M. Zurek, Phys. Rev. D **103**, 016006 (2021), 1909.09170.
- [37] R. M. Geilhufe, F. Kahlhoefer, and M. W. Winkler, Phys. Rev. D **101**, 055005 (2020), 1910.02091.
- [38] S. M. Griffin, Y. Hochberg, K. Inzani, N. Kurinsky, T. Lin, and T. Chin, Phys. Rev. D **103**, 075002 (2021), 2008.08560.
- [39] A. Prabhu and C. Blanco (2022), 2211.05787.
- [40] A. Esposito and S. Pavaskar, Phys. Rev. D **108**, L011901 (2023), 2210.13516.
- [41] Z.-L. Liang, L. Zhang, P. Zhang, and F. Zheng, JHEP **01**, 149 (2019), 1810.13394.
- [42] S. M. Griffin, K. Inzani, T. Trickle, Z. Zhang, and K. M. Zurek, Phys. Rev. D **104**, 095015 (2021), 2105.05253.
- [43] Y. Kahn and T. Lin, Rept. Prog. Phys. **85**, 066901 (2022), 2108.03239.
- [44] T. Trickle, Phys. Rev. D **107**, 035035 (2023), 2210.14917.
- [45] C. E. Dreyer, R. Essig, M. Fernandez-Serra, A. Singal, and C. Zhen (2023), 2306.14944.
- [46] S. Knapen, J. Kozaczuk, and T. Lin, Phys. Rev. D **104**, 015031 (2021), 2101.08275.
- [47] S. Knapen, J. Kozaczuk, and T. Lin, Phys. Rev. D **105**, 015014 (2022), 2104.12786.
- [48] Y. Hochberg, Y. Kahn, N. Kurinsky, B. V. Lehmann, T. C. Yu, and K. K. Berggren, Phys. Rev. Lett. **127**, 151802 (2021), 2101.08263.
- [49] N. Kurinsky, D. Baxter, Y. Kahn, and G. Krnjaic, Phys. Rev. D **102**, 015017 (2020), 2002.06937.
- [50] G. B. Gelmini, V. Takhistov, and E. Vitagliano, Phys. Lett. B **809**, 135779 (2020), 2006.13909.
- [51] J. Kozaczuk and T. Lin, Phys. Rev. D **101**, 123012 (2020), 2003.12077.
- [52] A. Mitridate, T. Trickle, Z. Zhang, and K. M. Zurek, JHEP **09**, 123 (2021), 2106.12586.
- [53] Z.-L. Liang, C. Mo, and P. Zhang, Phys. Rev. D **104**, 096001 (2021), 2107.01209.
- [54] K. Agashe, Y. Cui, L. Necib, and J. Thaler, JCAP **10**, 062 (2014), 1405.7370.
- [55] J. Berger, Y. Cui, and Y. Zhao, JCAP **02**, 005 (2015), 1410.2246.
- [56] K. Agashe, Y. Cui, L. Necib, and J. Thaler, J. Phys. Conf. Ser. **718**, 042041 (2016), 1512.03782.
- [57] L. Su, L. Wu, and B. Zhu (2023), 2308.02204.
- [58] J. Alvey, M. Campos, M. Fairbairn, and T. You, Phys. Rev. Lett. **123**, 261802 (2019), 1905.05776.
- [59] C. A. Argüelles, V. Muñoz, I. M. Shoemaker, and V. Takhistov, Phys. Lett. B **833**, 137363 (2022), 2203.12630.
- [60] L. Darmé, Phys. Rev. D **106**, 055015 (2022), 2205.09773.
- [61] H. An, M. Pospelov, J. Pradler, and A. Ritz, Phys. Rev. Lett. **120**, 141801 (2018), [Erratum: Phys.Rev.Lett. 121, 259903 (2018)], 1708.03642.
- [62] T. Emken, Phys. Rev. D **105**, 063020 (2022), 2102.12483.
- [63] H. An, H. Nie, M. Pospelov, J. Pradler, and A. Ritz, Phys. Rev. D **104**, 103026 (2021), 2108.10332.
- [64] C. V. Cappiello, N. P. A. Kozar, and A. C. Vincent (2022), 2210.09448.
- [65] T. Bringmann and M. Pospelov, Phys. Rev. Lett. **122**, 171801 (2019), 1810.10543.
- [66] Y. Ema, F. Sala, and R. Sato, Phys. Rev. Lett. **122**, 181802 (2019), 1811.00520.
- [67] C. V. Cappiello and J. F. Beacom, Phys. Rev. D **100**, 103011 (2019), [Erratum: Phys.Rev.D 104, 069901 (2021)], 1906.11283.
- [68] W. Wang, L. Wu, J. M. Yang, H. Zhou, and B. Zhu, JHEP **12**, 072 (2020), [Erratum: JHEP 02, 052 (2021)], 1912.09904.
- [69] S.-F. Ge, J. Liu, Q. Yuan, and N. Zhou, Phys. Rev. Lett. **126**, 091804 (2021), 2005.09480.
- [70] G. Guo, Y.-L. S. Tsai, M.-R. Wu, and Q. Yuan, Phys. Rev. D **102**, 103004 (2020), 2008.12137.
- [71] C. Xia, Y.-H. Xu, and Y.-F. Zhou, Nucl. Phys. B **969**, 115470 (2021), 2009.00353.
- [72] Y. Ema, F. Sala, and R. Sato, SciPost Phys. **10**, 072 (2021), 2011.01939.
- [73] J.-C. Feng, X.-W. Kang, C.-T. Lu, Y.-L. S. Tsai, and F.-S. Zhang, JHEP **04**, 080 (2022), 2110.08863.
- [74] W. Wang, L. Wu, W.-N. Yang, and B. Zhu (2021), 2111.04000.
- [75] X. Cui et al. (PandaX-II), Phys. Rev. Lett. **128**, 171801 (2022), 2112.08957.
- [76] R. Xu et al. (CDEX), Phys. Rev. D **106**, 052008 (2022), 2201.01704.
- [77] C. Xia, Y.-H. Xu, and Y.-F. Zhou, Phys. Rev. D **107**, 055012 (2023), 2206.11454.
- [78] T. N. Maity and R. Laha (2022), 2210.01815.
- [79] M. J. Boschini et al., Astrophys. J. **854**, 94 (2018), 1801.04059.
- [80] P. Adari et al. (SENSEI) (2023), 2312.13342.
- [81] X. Collaboration, *XENON1T S2-only data release* (2020), URL <https://doi.org/10.5281/zenodo.4075018>.
- [82] Z.-L. Liang and P. Zhang, JCAP **12**, 009 (2023), 2307.08546.
- [83] B. A. Cervantes-Vergara et al. (Oscura) (2023), 2304.04401.
- [84] P. Nozières and D. Pines, Phys. Rev. **113**, 1254 (1959), URL <https://link.aps.org/doi/10.1103/PhysRev.113.1254>.
- [85] V. V. Flambaum, L. Su, L. Wu, and B. Zhu, Sci. China Phys. Mech. Astron. **66**, 271011 (2023), 2012.09751.
- [86] R. Catena, T. Emken, N. A. Spaldin, and W. Tarantino, Phys. Rev. Res. **2**, 033195 (2020), 1912.08204.

Supplemental Material:

Plasmon-enhanced Direct Detection of Cosmic Rays Boosted Dark Matter

Zheng-Liang Liang,¹ Liangliang Su,² Lei Wu,² and Bin Zhu,³

¹College of Mathematics and Physics, Beijing University of Chemical Technology, Beijing, 100029, China

²Department of Physics and Institute of Theoretical Physics, Nanjing Normal University, Nanjing, 210023, China

³Department of Physics, Yantai University, Yantai 264005, China

In this supplemental material, we show the cross section of electronic excitation in semiconductor targets, the event rate induced by CRDM in semiconductors, and the electronic excitation in Xenon1T experiment.

CROSS SECTION OF ELECTRONIC EXCITATION IN SEMICONDUCTOR TARGETS

Here we fill up the details in the derivation that leads to the total cross section of DM-electron scattering in a semiconductor as the following,

$$\begin{aligned}
\sigma &= \sum_{i,f} \mathcal{P}_i \sigma_{i \rightarrow f} \\
&= \int \frac{d^3 p'_\chi}{(2\pi)^3} \frac{1}{2} \sum_{s,s'} \bar{u}_{p'_\chi}^{s'} \gamma^0 u_{p_\chi}^s \bar{u}_{p_\chi}^s \gamma^0 u_{p'_\chi}^{s'} \frac{2\pi\delta(\omega_{pp'} - \omega)}{4E_\chi E'_\chi v_\chi} \sum_{i,f} \mathcal{P}_i \langle i | e^{-i\mathbf{Q}\cdot\hat{\mathbf{x}}} | f \rangle \langle f | e^{i\mathbf{Q}\cdot\hat{\mathbf{x}}} | i \rangle \\
&= \int d\omega \delta(\omega + \varepsilon_i - \varepsilon_f) \int d^3\mathbf{Q} \delta^{(3)}(\mathbf{Q} + \mathbf{p}'_\chi - \mathbf{p}_\chi) \int \frac{d^3 p'_\chi}{(2\pi)^3} \frac{\pi \bar{\sigma}_{\chi e} [(E_\chi + E'_\chi)^2 - Q^2]}{4\mu_{\chi e}^2 E_\chi E'_\chi v_\chi} \left(\frac{\alpha^2 m_e^2 + m_{A'}^2}{Q^2 - \omega^2 + m_{A'}^2} \right)^2 \\
&\times 2\pi\delta(\omega_{pp'} - \omega) \int d^3\mathbf{x} d^3\mathbf{x}' \sum_{i,f} \mathcal{P}_i \langle i | e^{-i\mathbf{Q}\cdot\hat{\mathbf{x}}'} \hat{\rho}_e | f \rangle \langle f | e^{i\mathbf{Q}\cdot\hat{\mathbf{x}}} \hat{\rho}_e | i \rangle \\
&= \int d\omega \int \frac{d^3\mathbf{Q}}{(2\pi)^3} \frac{\pi \bar{\sigma}_{\chi e} [(E_\chi + E'_\chi)^2 - Q^2]}{4\mu_{\chi e}^2 E_\chi E'_\chi v_\chi} \left(\frac{\alpha^2 m_e^2 + m_{A'}^2}{Q^2 - \omega^2 + m_{A'}^2} \right)^2 2\pi\delta(\omega_{pp'} - \omega) \\
&\times \sum_{i,f} \mathcal{P}_i \langle i | \hat{\rho}_e | f \rangle \langle f | \hat{\rho}_{-\mathbf{Q}} | i \rangle \delta(\omega + \varepsilon_i - \varepsilon_f) \\
&= V_{\text{target}} \int d\omega \int \frac{d^3\mathbf{Q}}{(2\pi)^3} \frac{\pi \bar{\sigma}_{\chi e} [(E_\chi + E'_\chi)^2 - Q^2]}{4\mu_{\chi e}^2 E_\chi E'_\chi v_\chi} \left(\frac{\alpha^2 m_e^2 + m_{A'}^2}{Q^2 - \omega^2 + m_{A'}^2} \right)^2 \delta(\omega_{pp'} - \omega) S_{\hat{\rho}\hat{\rho}}(\mathbf{Q}, \omega) \\
&= 2V_{\text{target}} \int d\omega \int \frac{d^3\mathbf{Q}}{(2\pi)^3} \frac{\pi \bar{\sigma}_{\chi e} [(E_\chi + E'_\chi)^2 - Q^2]}{4\mu_{\chi e}^2 E_\chi E'_\chi v_\chi} \left(\frac{\alpha^2 m_e^2 + m_{A'}^2}{Q^2 - \omega^2 + m_{A'}^2} \right)^2 \frac{\delta(\omega_{pp'} - \omega)}{V_{\text{Cou}}(\mathbf{Q})} \text{Im} \left[\frac{-1}{\epsilon(\mathbf{Q}, \omega)} \right],
\end{aligned}$$

where $V_{\text{target}} = N_{\text{cell}} V_{\text{cell}}$ is the volume of the target material. In the third line, we insert two identities $\int d\omega \delta(\omega + \varepsilon_i - \varepsilon_f)$ and $\int d^3\mathbf{Q} \delta^{(3)}(\mathbf{Q} + \mathbf{p}'_\chi - \mathbf{p}_\chi)$ for the change of variables. In order to discuss the excitation process in the context of the response theory, we introduce the electron density operator $\hat{\rho}_e(\mathbf{x}) \equiv \hat{\psi}_e^\dagger(\mathbf{x}) \hat{\psi}_e(\mathbf{x})$, where the nonrelativistic field operator $\hat{\psi}_e(\mathbf{x}) = \sum_j \hat{a}_j u_j(\mathbf{x})$ is expressed in terms of the eigen wavefunctions $\{u_j(\mathbf{x})\}$ and their corresponding creation (annihilation) operators $\{\hat{a}_j^\dagger\}$ ($\{\hat{a}_j\}$). In the momentum space, the density operator is rewritten as $\rho_{\mathbf{Q}} \equiv \int d^3\mathbf{x} \hat{\rho}_e(\mathbf{x}) e^{-i\mathbf{Q}\cdot\hat{\mathbf{x}}}$, which describes the density fluctuation of the electron system [84]. The dynamic structure factor is defined as

$$S_{\hat{\rho}\hat{\rho}}(\mathbf{Q}, \omega) = \frac{2\pi}{V_{\text{target}}} \sum_{i,f} \mathcal{P}_i |\langle f | \hat{\rho}_{-\mathbf{Q}} | i \rangle|^2 \delta(\omega + \varepsilon_i - \varepsilon_f) \quad (\text{S.1})$$

$$= i \frac{[\chi_{\hat{\rho}\hat{\rho}}(\mathbf{Q}, \omega + i0^+) - \chi_{\hat{\rho}\hat{\rho}}(\mathbf{Q}, \omega - i0^+)]}{1 - e^{-\beta\omega}} \quad (\text{S.2})$$

$$\simeq i [\chi_{\hat{\rho}\hat{\rho}}(\mathbf{Q}, \omega + i0^+) - \chi_{\hat{\rho}\hat{\rho}}(\mathbf{Q}, \omega - i0^+)] \quad (\text{S.3})$$

$$= -2 \operatorname{Im} [\chi_{\hat{\rho}\hat{\rho}}^r(\mathbf{Q}, \omega)] \quad (\text{S.4})$$

$$= \frac{2}{V_{\text{Cou}}(\mathbf{Q})} \operatorname{Im} \left[\frac{-1}{\epsilon(\mathbf{Q}, \omega)} \right], \quad (\text{S.5})$$

where $1 - e^{-\beta\omega}$ depends on the inverse temperature $\beta = 1/k_B T$, which can be approximated as 1 for the semiconductor target. The master function $\chi_{\hat{\rho}\hat{\rho}}(\mathbf{Q}, z)$, representing the correlation function of density operator $\hat{\rho}\hat{\rho}$, can be estimated by the Matsubara Green's function, and $\chi_{\hat{\rho}\hat{\rho}}^r(\mathbf{Q}, \omega) = \chi_{\hat{\rho}\hat{\rho}}(\mathbf{Q}, \omega + i0^+)$ and $\chi_{\hat{\rho}\hat{\rho}}(\mathbf{Q}, \omega - i0^+)$ are the corresponding retarded and advanced correlation function. For the last line, we use the relation between the dielectric function and retarded correlation function in the linear response theory, that is

$$\frac{1}{\epsilon(\mathbf{Q}, \omega)} = 1 + V_{\text{Cou}}(\mathbf{Q}) \chi_{\hat{\rho}\hat{\rho}}^r(\mathbf{Q}, \omega). \quad (\text{S.6})$$

In the nonrelativistic limit, the cross section in Eq. (S.1) reduces to the expression in Ref. [53], which describes the scattering between a halo DM particle and the electrons in solids.

EVENT RATE INDUCED BY CRDM IN SEMICONDUCTOR

In this section, we provide a detailed derivation of the excitation event rate in semiconductors induced by a relativistic DM flux. Because the semiconductor target can be regarded as isotropic (i.e., $\operatorname{Im} [-\epsilon^{-1}(\omega, Q)]$ is independent of the direction of \mathbf{Q}), we take the direction of initial momentum \mathbf{p}_χ as the z -axis of the spherical coordinate system and integrate out the polar angle of \mathbf{Q} with respect to \mathbf{p}_χ , so we have

$$\begin{aligned} R &= \frac{1}{M_{\text{target}}} \int d\omega \int dE_\chi \int \frac{d\Omega}{4\pi} \frac{d\Phi_\chi}{dE_\chi} \frac{d\sigma}{d\omega} \\ &= \frac{2}{\rho_T} \frac{\pi \bar{\sigma}_{\chi e}}{\mu_{\chi e}^2} \int d\omega \int dE_\chi \frac{d\Phi(E_\chi)}{dE_\chi} \int \frac{d \cos \theta_{\mathbf{Q}\mathbf{p}_\chi} d\phi}{4\pi} \int \frac{d^3\mathbf{Q}}{(2\pi)^3} \frac{(E_\chi + E'_\chi)^2 - Q^2}{4E_\chi E'_\chi} \left(\frac{\alpha^2 m_e^2 + m_{A'}^2}{Q^2 - \omega^2 + m_{A'}^2} \right)^2 \\ &\quad \times \frac{Q^2}{4\pi\alpha} \frac{E_\chi}{p_\chi} \operatorname{Im} \left[\frac{-1}{\epsilon(\mathbf{Q}, \omega)} \right] \delta(E'_\chi - E_\chi + \omega) \Big|_{E'_\chi = \sqrt{|\mathbf{p}'_\chi|^2 + m_e^2}; \mathbf{p}'_\chi = \mathbf{p}_\chi - \mathbf{Q}} \\ &= \frac{1}{\rho_T} \frac{\bar{\sigma}_{\chi e}}{4\alpha\mu_{\chi e}^2} \int d\omega \int \frac{d^3\mathbf{Q}}{(2\pi)^3} \int dE_\chi \frac{d\Phi(E_\chi)}{dE_\chi} \int_{E^-(p_\chi)}^{E^+(p_\chi)} \left| \frac{d \cos \theta_{\mathbf{Q}\mathbf{p}_\chi}}{dE'_\chi} \right| dE'_\chi \frac{Q^2 E_\chi}{p_\chi} \frac{(E_\chi + E'_\chi)^2 - Q^2}{4E_\chi E'_\chi} \\ &\quad \times \left(\frac{\alpha^2 m_e^2 + m_{A'}^2}{Q^2 - \omega^2 + m_{A'}^2} \right)^2 \operatorname{Im} \left[\frac{-1}{\epsilon(\mathbf{Q}, \omega)} \right] \delta(E'_\chi - E_\chi + \omega) \\ &= \frac{1}{\rho_T} \frac{\bar{\sigma}_{\chi e}}{4\alpha\mu_{\chi e}^2} \int d\omega \int \frac{d^3\mathbf{Q}}{(2\pi)^3} \int dE_\chi \frac{d\Phi(E_\chi)}{dE_\chi} \int_{E^-(p_\chi)}^{E^+(p_\chi)} dE'_\chi \left(\frac{E_\chi E'_\chi Q}{p_\chi^2} \right) \frac{(E_\chi + E'_\chi)^2 - Q^2}{4E_\chi E'_\chi} \\ &\quad \times \left(\frac{\alpha^2 m_e^2 + m_{A'}^2}{Q^2 - \omega^2 + m_{A'}^2} \right)^2 \operatorname{Im} \left[\frac{-1}{\epsilon(\mathbf{Q}, \omega)} \right] \delta(E'_\chi - E_\chi + \omega) \\ &= \frac{1}{\rho_T} \frac{\bar{\sigma}_{\chi e}}{4\alpha\mu_{\chi e}^2} \int d\omega \int \frac{d^3\mathbf{Q}}{(2\pi)^3} \int dE_\chi \frac{d\Phi(E_\chi)}{dE_\chi} \left(\frac{E_\chi(E_\chi - \omega)}{p_\chi^2} \right) \frac{(2E_\chi - \omega)^2 - Q^2}{4E_\chi(E_\chi - \omega)} \left(\frac{\alpha^2 m_e^2 + m_{A'}^2}{Q^2 - \omega^2 + m_{A'}^2} \right)^2 \\ &\quad \times Q \operatorname{Im} \left[\frac{-1}{\epsilon(\mathbf{Q}, \omega)} \right] \Theta[E_\chi - E^- - \omega], \end{aligned} \quad (\text{S.7})$$

where $E^\pm(p_\chi) = \sqrt{(p_\chi \pm Q)^2 + m_\chi^2}$ with $p_\chi = |\mathbf{p}_\chi|$. In the above derivation, we take a variable transformation from $\cos\theta_{\mathbf{p}_\chi\mathbf{Q}}$ to $E_{p'_\chi}$, along with its corresponding Jacobian

$$\left| \frac{d \cos\theta_{\mathbf{p}_\chi\mathbf{Q}}}{dE'_{p_\chi}} \right| = \left(\frac{E'_\chi}{p_\chi Q} \right), \quad (\text{S.8})$$

and the step function in the last line indicates whether the span of integration over $E_{p'_\chi}$ covers the zero in the delta function. In addition, if the DM flux is rewritten with the speed distribution function, $\int dE_\chi d\Phi(E_\chi)/dE_\chi = (\rho_\chi/m_\chi) \int d^3v v_\chi f_\chi(\mathbf{v}_\chi)$, the Eq. (S.7) can spontaneously reduce to the Eq. (13) in Ref. [46] for a nonrelativistic DM flux.

ELECTRONIC EXCITATION IN XENON1T EXPERIMENT

The differential event rate of DM-electron scattering in xenon1T experiment is given by [4, 25]

$$\frac{dR_{\text{ion}}}{d \ln \Delta E_e} = N_T \Phi_{\text{halo}} \frac{d \langle \sigma_{\text{ion}} v \rangle}{d \ln \Delta E_e} \quad (\text{S.9})$$

here N_T is the number density of target nuclei and Φ_{halo} is the flux of DM halo. The deposit energy $\Delta E_e = E_R + |E_{nl}|$ is the function of the binding energy of (n, l) shell E_{nl} and the final electron energy $E_R = k'^2/2m_e$. The thermally averaged differential cross section $\frac{d \langle \sigma_{\text{ion}} v \rangle}{d \ln \Delta E_e}$ can be obtained by

$$\frac{d \langle \sigma_{\text{ion}}^i v \rangle}{d \ln \Delta E_e} = \frac{\bar{\sigma}_e}{8\mu_{\chi e}^2} \int Q dQ |f_{\text{ion}}^i(k', Q)|^2 |F_{\text{DM}}(q)|^2 \eta(E_{\text{min}}) \quad (\text{S.10})$$

where $|f_{\text{ion}}^i(k', Q)|^2$ is the ionization form factor, which describes an electron with initial state (n, l) excited the continuum state with momentum k' , and we adopted the results of Ref. [85, 86] in this work. The momentum-dependent form factor $|F_{\text{DM}}|^2$ is defined by

$$\begin{aligned} |F_{\text{DM}}(q)|^2 &= \frac{|\overline{\mathcal{M}_{\text{free}}}|^2}{|\mathcal{M}_{\text{free}}(\alpha m_e)|^2} \\ &= \frac{(\alpha^2 m_e^2 + m_{A'}^2)^2}{(q^2 + m_{A'}^2)^2} \frac{8m_e^2 E_\chi^2 + q^4 - 2q^2(m_\chi^2 + m_e^2 + 2m_e E_\chi)}{8m_e^2 m_\chi^2}, \end{aligned} \quad (\text{S.11})$$

where q is the four transfer momentum with $q^2 = Q^2 - \Delta E_e^2$.

The η function includes the CRDM flux, i.e., $\eta(E_{\text{min}}) = \int_{E_{\text{min}}} dE_\chi \Phi_{\text{halo}}^{-1} \frac{m_\chi^2}{p_\chi^2} \frac{d\Phi_\chi}{dE_\chi}$, which is consistent with the nonrelativistic form in Ref. [4](see supplemental material in Ref. [85]). E_{min} is the minimum DM energy to obtain an electron with E_R by DM-electron scattering,

$$p_\chi^{\text{min}} = \frac{Q}{2(1 - \Delta E_e^2/Q^2)} \left(1 - \frac{\Delta E_e^2}{Q^2} + \frac{\Delta E_e}{Q} \sqrt{\left(1 - \frac{\Delta E_e^2}{Q^2} \right) \left(1 - \frac{\Delta E_e^2}{Q^2} + \frac{4m_\chi^2}{Q^2} \right)} \right). \quad (\text{S.12})$$

In general, the experimental observation signal is the number of photoelectrons (PE), and we need to make a transform, i.e.,

$$\frac{dR_{\text{ion}}}{dS2} = \int dE_e \epsilon(S2) P(S2 | \Delta E_e) \frac{dR_{\text{ion}}}{d\Delta E_e}, \quad (\text{S.13})$$

where $\epsilon(S2)$ is the detector efficiency. $P(S2 | \Delta E_e)$ represents the probability function that converts deposited energy into the PE numbers for the S2 signal, as well as their product is tabulated by XENON1T collaboration in Ref. [81]. In this work, we consider an S2 region of interest PE $\in [165.3, 271.7]$ and the derived limits of 24.6 signal events with 0.97678 tonne \cdot year exposure.